Journal of Medicinal Chemistry

Article

pubs.acs.org/jmc

# Preparation and Evaluation of Fluorine-18-Labeled Insulin as a Molecular Imaging Probe for Studying Insulin Receptor Expression in Tumors

Dong Hyun Kim,[†] Megan Blacker,[‡] and John F. Valliant*[,†,‡]

[†]Department of Chemistry and Chemical Biology and [‡]Centre for Probe Development and Commercialization, McMaster University, 1280 Main Street West, Hamilton, Ontario, Canada L8S 4M1

Supporting Information

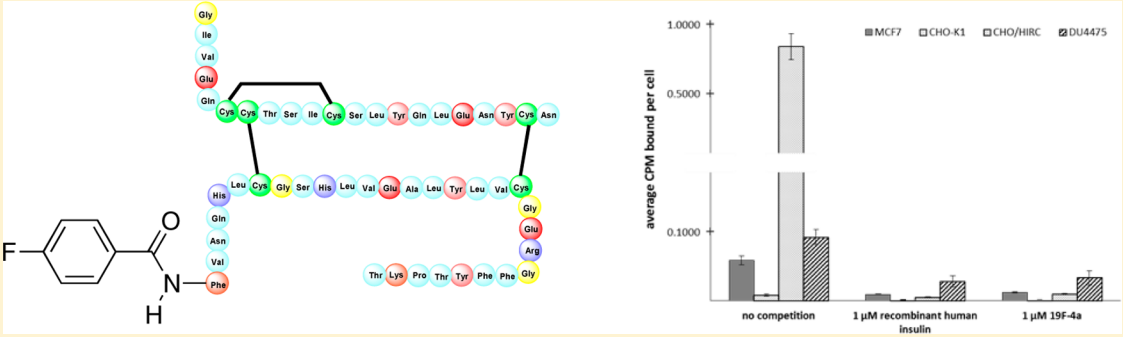


**ABSTRACT:** A convenient emulsion-based labeling method was used to synthesize fluorine-18-labeled insulin specifically $B^1$-(4-[$^{18}$F]fluorobenzoyl)insulin ($^{18}$F-**4b**) in 6% overall radiochemical yield in 240 min. In vitro screening in MCF7 breast cancer cells demonstrated that the nonradioactive analogue $^{19}$F-**4a** effectively competed with $^{125}$I-insulin for the insulin receptor ($IC_{50}$ = 10.6 nM) comparable to that for insulin ($IC_{50}$ = 7.4 nM). $^{18}$F-**4b** was also more stable than $^{125}$I-insulin in mouse plasma with 50% remaining intact after 30 min. A biodistribution study in normal mice showed initial uptake of the tracer in the kidneys, liver, and gall bladder but rapid clearance via the urine/bladder which was also observed in murine models bearing insulin receptor positive tumors.

## INTRODUCTION

Insulin, a peptide-based hormone discovered more than 90 years ago,[1] plays a critical role in regulating carbohydrate and fat metabolism for energy homeostasis.[2] Dysregulation of the insulin system plays a critical role in the etiology of a wide variety of diseases beyond diabetes including obesity, atherosclerosis, hypertension,[3] heart failure,[4] neurodegenerative disease,[5] and cancer.[6] For the latter, the insulin receptor (IR) and insulin-like growth factor-1 receptor (IGF-1R) are highly overexpressed on the surface of a wide array of different cancers including hepatocellular carcinomas,[7] breast cancer,[8] and pancreatic cancer[9] where the IR/IGF-1R axis is an active target for drug development.[10]

The ability to monitor changes in IR expression in vivo could be used to detect neoplastic lesions and as a means to identify treatment-resistant tumors. There is increasing evidence that anti-IGF therapies work best on tumors that have low IR expression; consequently, the ability to assess IR levels would be a valuable tool to guide patient selection.[11] A radiolabeled probe derived from insulin is one approach being explored for measuring changes in IR levels in vivo. One advantage of this class of radiopharmaceuticals is that in addition to their utility in oncology they could also be used to assess new protein delivery mechanisms and different formulations of insulin for use in treating diabetes.

$^{125}$I-Insulin, which carries the isotope at the $A^{14}$ tyrosine residue, is used extensively to study insulin biochemistry; however, the radioactive emission (electron capture, $E$ = 35 keV) is not ideal for imaging.[12] Iodine-123[13] and iodine-124[14] analogues have been developed and shown to be effective mimetics of $^{125}$I-insulin in both preclinical and clinical studies. A more attractive option with respect to imaging properties and isotope availability and cost would be an insulin analogue labeled with $^{18}$F which is the most widely used PET isotope in diagnostic medicine.

Fluorine-18-labeled insulin carrying a prosthetic group at the $B^1$ site has been reported;[15] however, the associated radiolabeling methods were cumbersome and low yielding. Furthermore, none of the reported agents were evaluated in tumor cells or the associated mouse models. Here we report the use of a new emulsion labeling method to produce high purity $^{18}$F-radiolabeled insulin that is capable of binding the IR. The product was evaluated in vitro using a series of cancer cell lines and its utility as a tumor-seeking radiopharmaceutical evaluated in direct comparison to $^{125}$I-labeled insulin.

**Received:** July 5, 2013

   dx.doi.org/10.1021/jm401020c | J. Med. Chem. XXXX, XXX, XXX−XXX

## RESULTS AND DISCUSSION

**Synthesis.** The initial step involved the preparation of the nonradioactive analogue of the target material as a reference standard for the tracer level synthesis and as a means to assess the ability of the construct to bind the IR in vitro. The $B^1$ amino acid of insulin was selected as the site for linking the prosthetic group because it has been shown that derivatization of the phenylalanine at the N-terminus of the B-chain ($PheB^1$) does not impact receptor binding affinity or the ability to stimulate glucose uptake.[15b,16] Because the $GlyA^1$ and $LysB^{29}$ amino groups of insulin are the most nucleophilic, prior to bioconjugation these groups were protected as *tert*-butyloxycarbonyl (Boc) carbamates. $A^1,B^{29}$-di(*tert*-butyloxycarbonyl)insulin (DBI) was prepared using a previously reported procedure[15b,c] and purified by semipreparative HPLC. Following freeze-drying, the resulting product was desalted via size exclusion chromatography (SEC), which is a critical step for ensuring that the modified protein will react with active esters. After lyophilization to remove the buffer employed during SEC, the desired product was obtained in good yield (61%) and HPLC and MS data matched that reported in the literature.

4-Fluorobenzoate was used as the prosthetic group because of its small size, which should minimize perturbation of receptor and nontarget protein binding. Furthermore, *N*-succinimidyl-4-fluorobenzoate (SFB) is a convenient and effective reagent to label amino groups in both proteins and a variety of other biomolecules with $^{18}F$.[17] $A^1,B^{29}$-di(*tert*-butyloxycarbonyl)-$B^1$-(4-fluorobenzoyl)insulin (**1**) was synthesized by combining DBI with the $^{19}F$-SFB ($^{19}F$-**2a**) in the presence of 5% $Et_3N$ in DMSO (Scheme 1). After 1.5 h, precipitation was induced using

**Scheme 1. Synthesis of Reference Standard 4a**

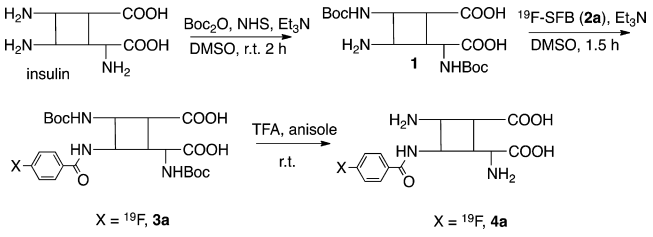


cold ether and the desired product isolated by HPLC in 57% yield. Deprotection of the Boc groups at $GlyA^1$ and $LysB^{29}$ was carried out using TFA containing 5% anisole and $^{19}F$-**4a** isolated using semipreparative HPLC. The overall yield of compound $^{19}F$-**4a** was 39% from DBI, and the purity was greater than 95% as determined by HPLC-MS.

**In Vitro Screening.** A series of Western blots were run on tumor lysates derived from tumor xenografts made from common human cancer cell lines to assess relative IR expression levels and to select a candidate cell line for further screening of $^{19}F$-**4a** (Figure 1). Of the 13 xenografts tested at equivalent protein loadings (50 $\mu$g), MeWo (malignant melanoma), SK-N-MC (neuroblastoma), and DU4475 and MDA-MB-231 (breast cancer) tumors appear to have the highest levels of IR protein. This was followed closely by MCF7 (breast cancer) grown in the presence of estrogen ($E_2$) pellet implants and LNCaP (prostate cancer) tumors. Transfected cell lines are often used to screen new candidate molecular imaging probes;[18] consequently, Chinese hamster ovary (CHO) cells stably transfected with the human insulin receptor isoform B (CHO/HIRC) were evaluated. These cells had significantly higher IR expression levels than all other cell lines, providing a convenient platform for further evaluation of **4a**/**b** both in vitro and in vivo (vide infra).

As an initial screen, the ability of insulin and $^{19}F$-**4a** to inhibit $^{125}I$-insulin binding to MCF7, DU4475, CHO-K1, and CHO/HIRC cells was evaluated, and the data were normalized by the number of cells incubated (Figure 2A,B). At both 0.1 nM and 1 nM $^{125}I$-insulin, there was measurable binding in all cell lines tested. The extent of binding was decreased to similar levels when incubated in the presence of recombinant human insulin or $^{19}F$-**4a** (1 $\mu$M). With the transfected cell line incubated with 1 nM $^{125}I$-insulin, the decrease in binding with recombinant human insulin was 99.4% while for $^{19}F$-**4a** it was 98.9%.

To better quantify the ability of $^{19}F$-**4a** to bind to the IR, competition binding assays with $^{125}I$-insulin (1 nM) were performed using MCF-7 cells. The average $IC_{50}$ for $^{19}F$-**4a** was 10.6 nM where at the 95% confidence interval (CI) the value ranged between 7.5 and 14.9 nM (Figure 3). This was similar to that observed for recombinant human insulin (7.4 nM; 95% CI: 5.4 to 10.2 nM). The affinity of $^{19}F$-**4a** compared to insulin for binding to the insulin-like growth factor receptor (IGF-1R) was also evaluated. Here a competition binding assay using $^{125}I$-labeled IGF-1, $^{19}F$-**4a** or insulin, and MCF-7 cells was performed (see Supporting Information for results and methods). The $IC_{50}$ for insulin was 44.5 nM (95% CI: 23.8 nM to 83.2 nM) while for $^{19}F$-**4a** the value was 52.3 nM (95% CI: 30.3 nM to 90.5 nM). These results confirm that $^{19}F$-**4a** has higher affinity for IR than for IGF-1R and that the addition of 4-fluorobenzoic acid to the $B^1$ position had little effect on the ability of the conjugate to bind to either receptor compared to native insulin.

**Radiochemistry.** Synthesis of $^{18}F$-**4b** involved the preparation of $^{18}F$-**2b** followed by coupling the active ester to DBI using a new water-in-oil emulsion method. For $^{18}F$-**2b**,[19] ethyl 4-trimethylammonium benzoate trifluoromethanesulfonate **5** was combined with [$^{18}F$]KF in DMSO (prepared following azeotropic drying of a $CH_3CN$ solution containing $KHCO_3$ and Kryptofix K-222) and the reaction mixture heated to 90 °C for 10 min to give ethyl 4-[$^{18}F$]fluorobenzoate, which was immediately hydrolyzed using 0.5 N NaOH (Scheme 2). The solution was subsequently diluted with water prior to passing the reaction mixture through a C18 SPE cartridge to remove DMSO and to separate the desired product from polar impurities. The active ester $^{18}F$-**2b** was prepared by adding *O*-(*N*-succinimidyl)-*N*,*N*,*N*′,*N*′-tetramethyluronium tetrafluoroborate (TSTU), followed by purification using semipreparative HPLC. $^{18}F$-**2b** was isolated in 45 ± 6% ($n$ = 9) decay-corrected radiochemical yield in greater than 95% purity where the total synthesis time including HPLC purification was 100 min.

We have shown previously that $^{18}F$-SFB will not react with DBI at the tracer level. This is likely a consequence of the low concentration of the active ester in solution based on the observation that the reaction at the macroscopic scale using equivalent amounts of DBI and $^{19}F$-SFB produced the desired product in high yield. To address this issue previously, a spacer group had to be incorporated to increase the reactivity of the amine. Recently however we reported that an emulsion-based labeling method could be used to increase the efficiency of labeling molecules with SFB and other prosthetic groups thereby negating the need to further modify the protein.[20]

Synthesis of $^{18}F$-**4b** (Scheme 3) was carried out using a water-in-oil emulsion prepared using isooctane. Isooctane containing the surfactant sorbitan monooleate (Span 80) was added to a vial containing $^{18}F$-SFB and DBI in a mixture of PBS (pH 7.4) and


dx.doi.org/10.1021/jm401020c | J. Med. Chem. XXXX, XXX, XXX−XXX

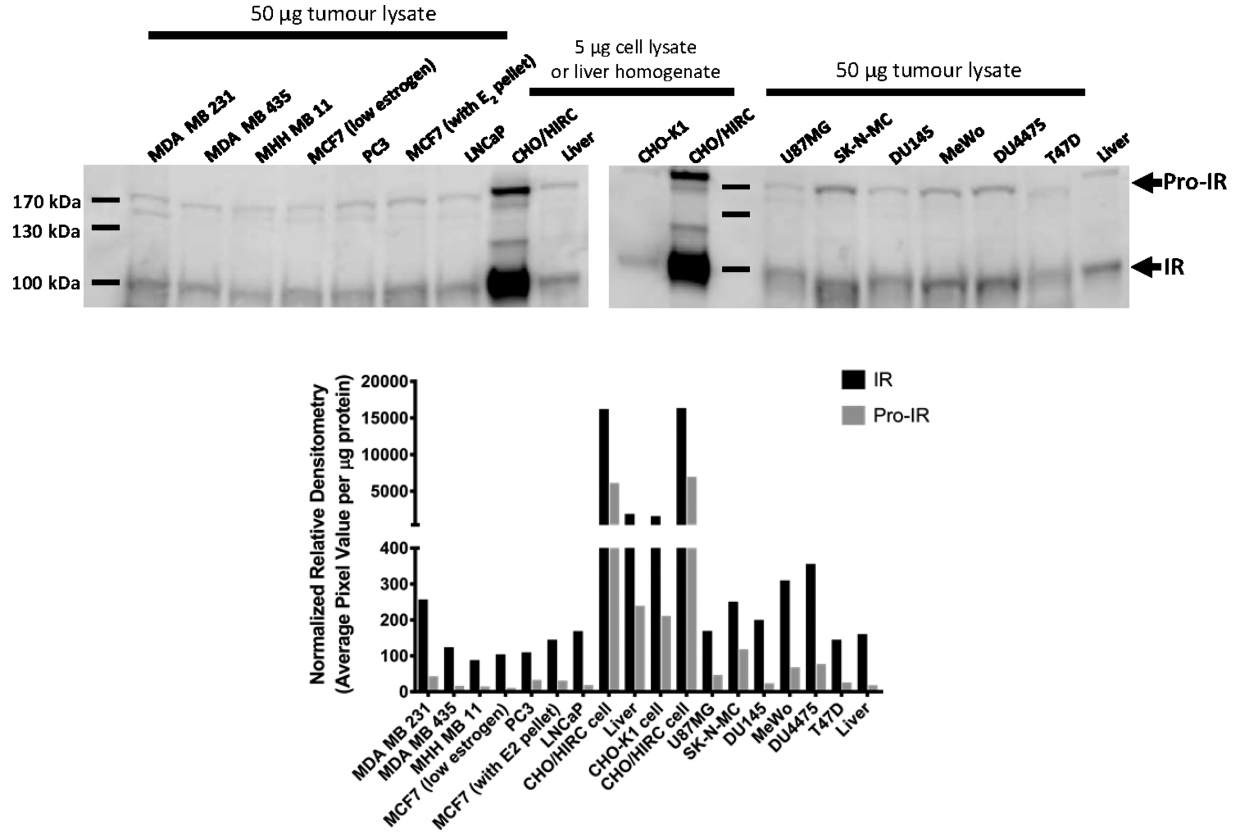


**Figure 1.** (Top) Western blot of tumor xenografts showing IR and pro-IR expression. For each tumor lysate, 50 $\mu$g of total protein was loaded per lane. CHO-K1 and CHO/HIRC cell lysates were also evaluated using 5 $\mu$g of total protein per lane. As a positive control for the antibody, 5 $\mu$g of total Balb/c mouse liver protein was loaded per lane (one lane per gel). (Bottom) Densitometry expressed as average pixel values per microgram of total protein loaded per lane for IR and Pro-IR specific bands.

0.1 M $NaHCO_3$ to create an emulsion. Subsequent vortexing at room temperature was followed by sonication for 30 min at room temperature with revortexing every 5 min. HPLC analysis of the reaction mixture showed three radioactive peaks, the desired product ($t_R$ = 7.9 min), 4-[$^{18}$F]fluorobenzoic acid ([$^{18}$F]FBA) ($t_R$ = 10 min) and unreacted [$^{18}$F]SFB ($^{18}$F-**2b**) ($t_R$ = 13 min) in a 6.5:2.5:1 ratio (Figure 4). It is important to note that conjugation following the same procedure including sonicating and vortexing in the absence of the emulsion failed to produce the desired product. TFA containing anisole was added to simultaneously break apart the emulsion and deprotect the Boc groups. The oil and water phases were separated by centrifugation for 10 min at 3500 rpm, and $^{18}$F-**4b** was isolated by semipreparative HPLC where the decay-corrected radiochemical yield of the conjugation and deprotection steps was 30 ± 10% ($n$ = 9).

The overall decay-corrected radiochemical yield of $^{18}$F-**4b** including radiochemical synthesis of [$^{18}$F]SFB was 6%, and the total synthesis time including HPLC purification was 240 min ($n$ = 9). The radiochemical purity of $^{18}$F-**4b** was >99% according to analytical HPLC analysis. The authenticity of the final product was confirmed by HPLC and coinjection with the authentic standard $^{19}$F-**4a**.

**Stability Studies.** The stability of $^{18}$F-**4b** was initially assessed in saline at 37 °C where the purity remained greater than 90% at 30 min. When incubated with mouse plasma at the same temperature, a single radiometabolite formed where after 30 min it represented nearly 50% of the sample (Figure 5). These results are consistent with literature reports of the rapid metabolism of iodinated-insulin derivatives, but it is noteworthy that for $^{125}$I-insulin the parent material degraded more rapidly than for $^{18}$F-**4b** in that it was effectively completely consumed after only 10 min.[14b,21] Given the positive imaging results previously obtained with iodinated insulin derivatives, the observed stability was deemed sufficient to warrant evaluating the radiotracer in vivo.

**Biodistribution of $^{18}$F-4b in Normal Mice.** Following administration of $^{18}$F-**4b** in the tail vein of Balb/c mice, there was 79.28 ± 17.62% ID/g in the kidneys at 5 min which decreased to 3.54 ± 0.83%ID/g by 30 min (Figure 6). Activity in the blood and heart decreased from 5.45 ± 0.56%ID/g and 2.27 ± 0.24% ID/g at 5 min to 0.43 ± 0.07 and 0.28 ± 0.05%ID/g at 30 min, respectively. There was substantial uptake in the gall bladder, reaching a maximum at 30 min (11.2 ± 1.60%ID/g) whereas there was no sustained uptake in the brain after 5 min. The majority of the activity resided in the urine/bladder where at 1 and 3 h postinjection the gall bladder was the only site with any significant amount of activity remaining.

**Biodistribution of $^{18}$F-4b in CHO/HIRC Tumor-Bearing Mice.** To evaluate the utility of the labeled hormone to seek out tumors overexpressing the IR, $^{18}$F-**4b** was administered to CD-1 nude mice that had been implanted with the CHO cells that had been transfected with the human IR (CHO/HIRC). Again blood clearance was rapid and decreased from 4.22 ± 0.78%ID/g at 5 min to 0.31 ± 0.05%ID/g at 30 min (Figure 7). The major uptake sites were gall bladder (15.47 ± 1.47%ID/g at 5 min; 2.20 ± 1.70%ID/g at 30 min), kidneys (52.73 ± 14.19%ID/g at 5 min; 3.91 ± 0.39%ID/g at 30 min), and urine/bladder where the preponderance of the activity resided. Tumor uptake was 1.74 ± 0.54%ID/g at 5 min and 0.30 ± 0.17%ID/g at 30 min.


dx.doi.org/10.1021/jm401020c | J. Med. Chem. XXXX, XXX, XXX−XXX

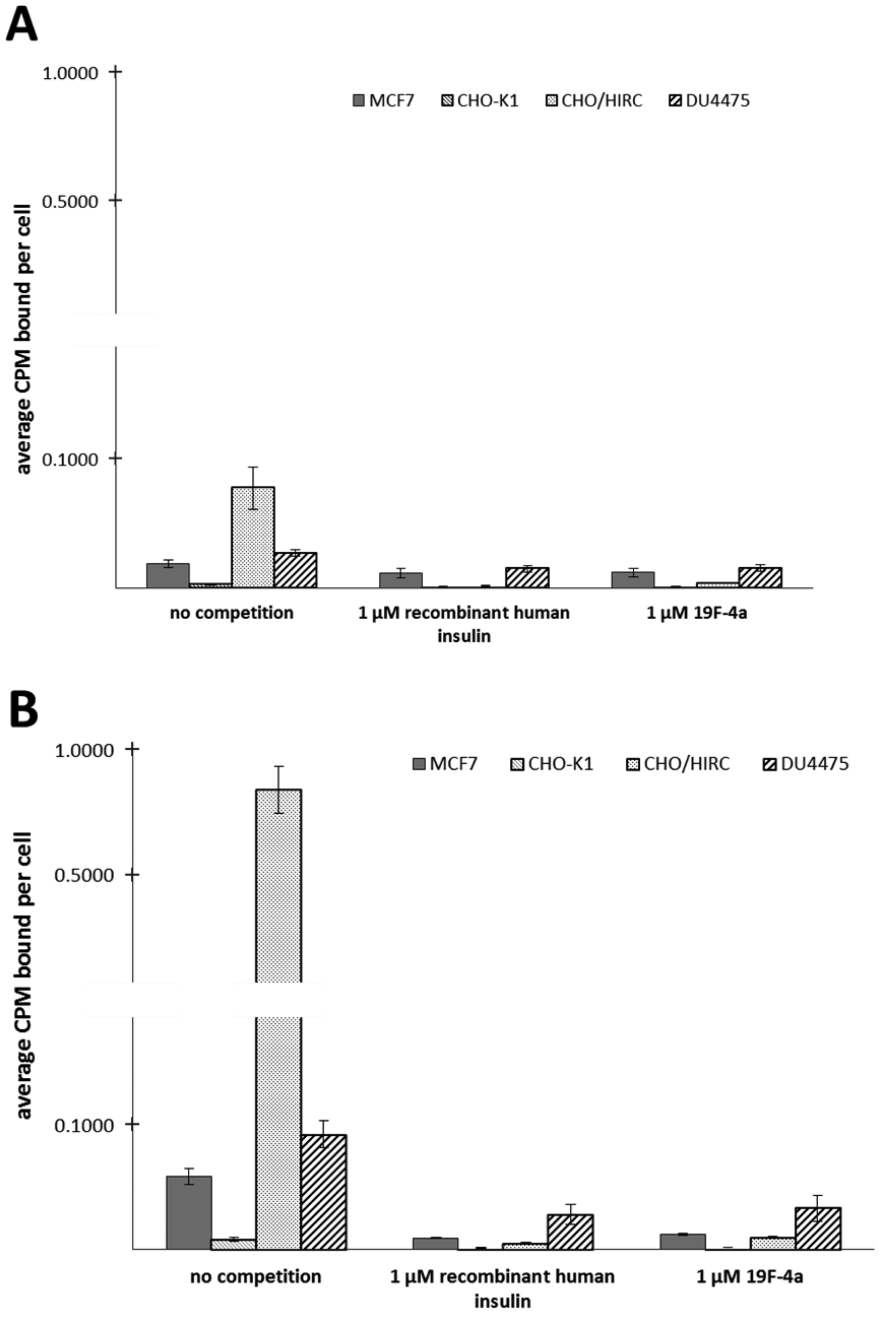


**Figure 2.** Binding of $^{125}$I-insulin (0.1 nM (A) and 1 nM (B)) to different IR-expressing cell lines in the presence or absence of 1 $\mu$M human recombinant insulin or $^{19}$F-**4a**.

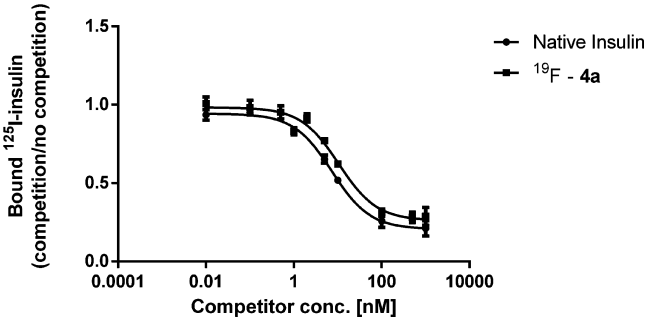


**Figure 3.** $^{125}$I-Insulin competition binding curves for recombinant human insulin and $^{19}$F-**4a**.

**Scheme 2. Radiochemical Synthesis of $^{18}$F-SFB (2b)**

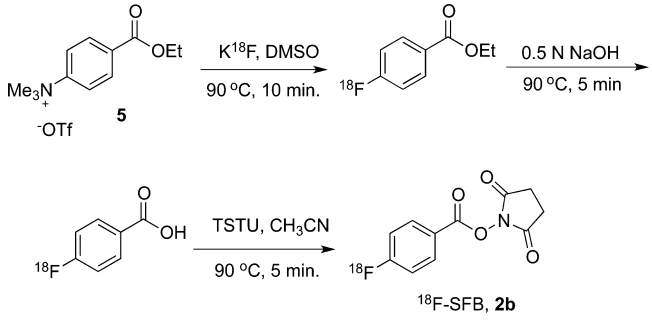



dx.doi.org/10.1021/jm401020c | J. Med. Chem. XXXX, XXX, XXX−XXX

**Scheme 3. Radiochemical Synthesis of $^{18}$F-Insulin ($^{18}$F-4b)**

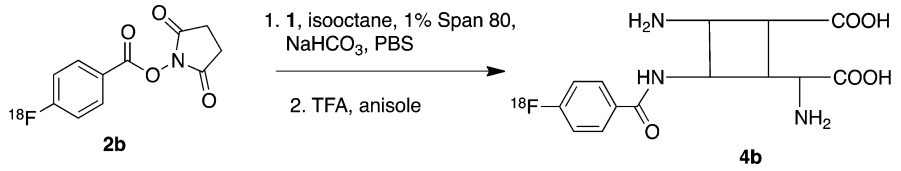


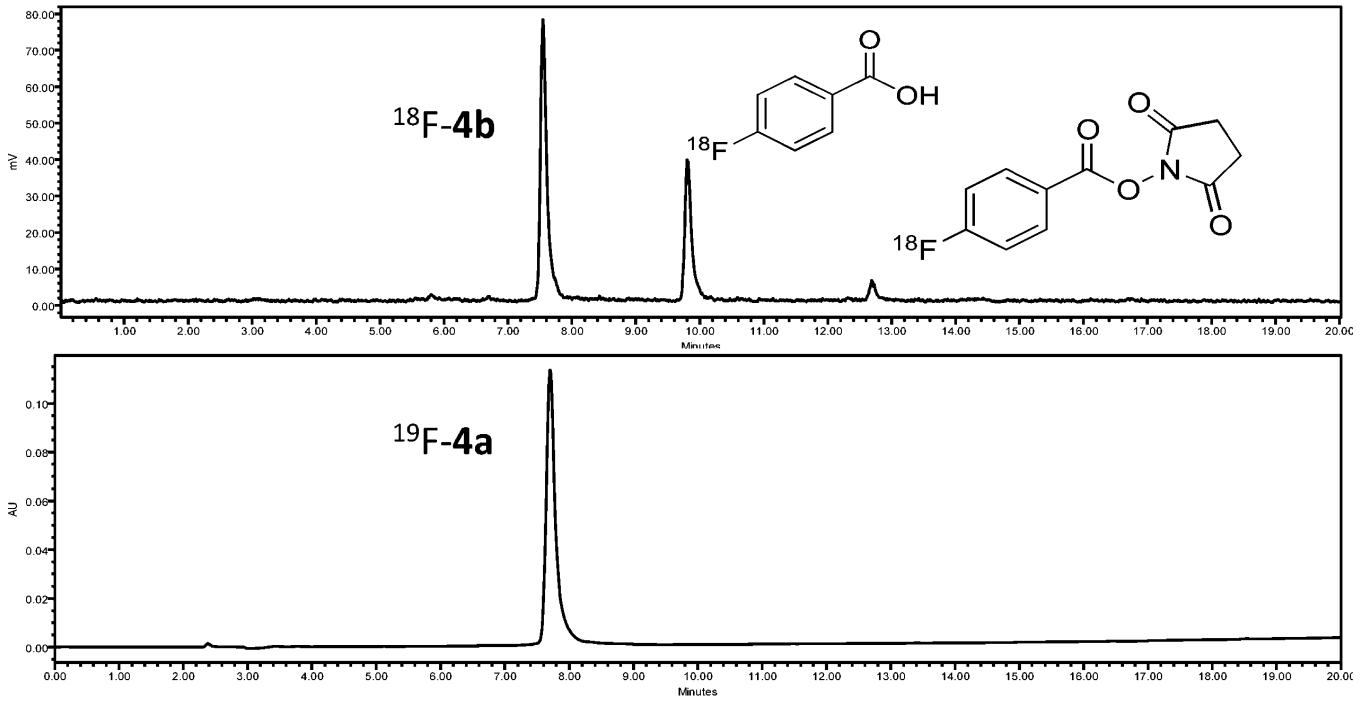


**Figure 4.** $\gamma$-HPLC chromatogram of the reaction mixture showing the presence of $^{18}$F-**4b**, [$^{18}$F]-4-fluorobenzoic acid, and $^{18}$F-SFB (top) and the UV-HPLC chromatogram of reference standard $^{19}$F-**4a**.

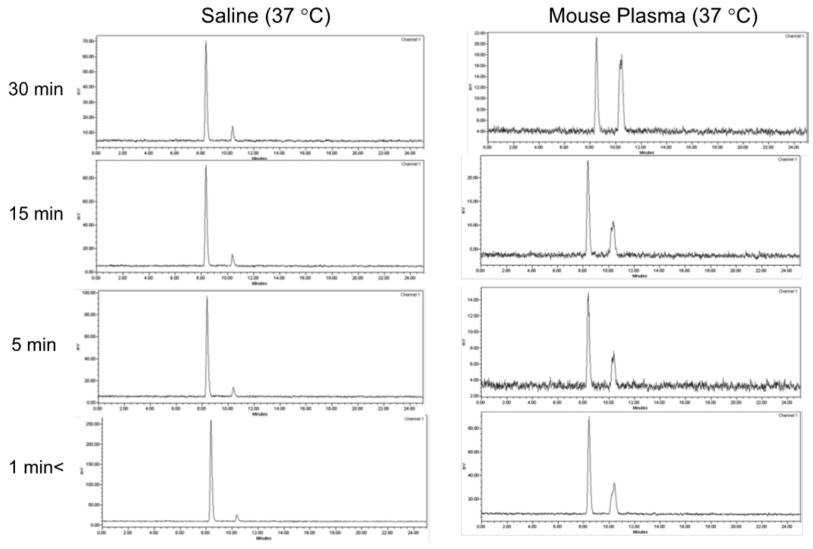


**Figure 5.** $\gamma$-HPLC chromatograms of $^{18}$F-**4b** following stability studies in saline and mouse plasma.

For comparison, the distribution of $^{125}$I-insulin in the same model was evaluated (Figure 8). Retention of the tracer in the blood and general organ uptake was typically higher than for $^{18}$F-**4b**. Tumor uptake increased from 1.43 ± 0.22%ID/g at 5 min to 5.02 ± 0.21%ID/g at 30 min; consequently, an additional time point was added to the study which showed that tumor uptake decreased to 3.43 ± 0.36%ID/g at 60 min. There was high initial uptake in the liver (16.08 ± 2.15% ID/g at 5 min; 2.30 ± 0.16% ID/g at 30 min) and kidneys (39.25 ± 3.06%ID/g at 5 min; 12.26 ± 1.90%ID/g at 30 min). Localization in the thyroid, which is evidence of deiodination, reached 20.77 ± 4.60%ID/g at 30 min.


dx.doi.org/10.1021/jm401020c | J. Med. Chem. XXXX, XXX, XXX−XXX

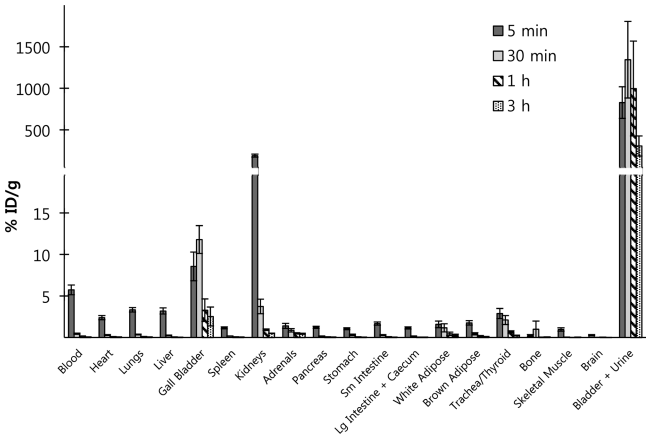


**Figure 6.** Biodistribution study of $^{18}$F-**4b** in Balb/c mice ($n$ = 5 per time point). The mice were administered ~0.91 MBq of $^{18}$F-**4b** (100 $\mu$L in PBS) via tail vein injection.

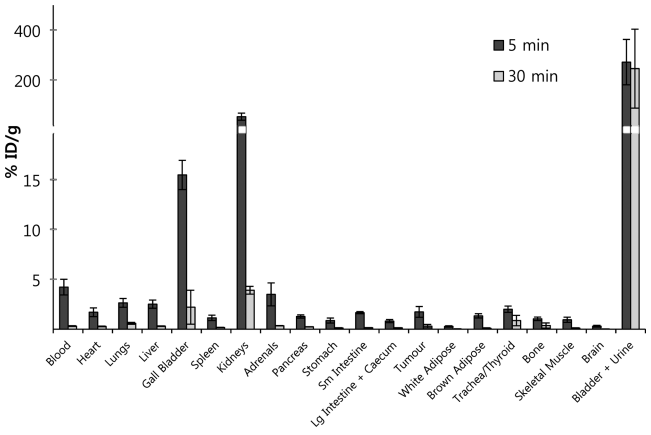


**Figure 7.** Biodistribution study of $^{18}$F-**4b** in CD-1 nude mouse model bearing (CHO/HIRC) tumors ($N$ = 3 per time point). The mice were administered ~0.68 MBq of $^{18}$F-**4b** (100 $\mu$L in PBS) via tail vein injection.

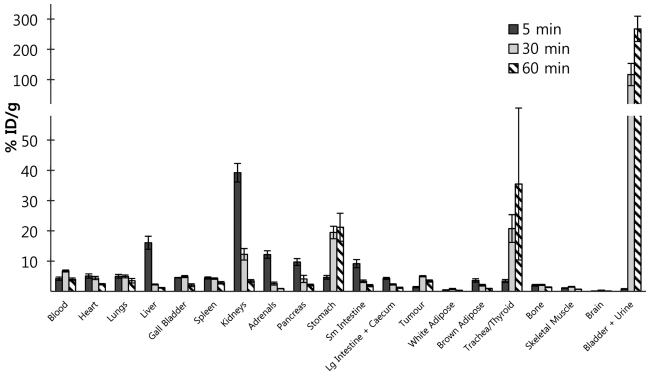


**Figure 8.** Biodistribution study of $^{125}$I-insulin in CD-1 nude mouse model bearing (CHO/HIRC) tumors ($N$ = 5 per time point). The mice were administered ~0.27 MBq of $^{125}$I-insulin in 150 $\mu$L via tail vein injection.

Despite the demonstrated ability of $^{18}$F-**4b** to bind to the IR and its reasonable stability profile, its uptake in IR-expressing tumors was not comparable to $^{125}$I-insulin, which is the current gold standard for evaluating insulin biochemistry in vitro and in vivo. From the biodistribution data it is apparent that the probe clears too rapidly and is not adequately retained in the tumor. Going forward it will be necessary to use a different prosthetic group that decreases the rate of elimination and increases blood circulation time while retaining the affinity and stability properties for $^{18}$F-**4b**.

## CONCLUSIONS

The preparation of a new radiolabeled analogue of insulin was reported. A convenient emulsion-based labeling method was used to produce the desired compound in high purity. In vitro screening demonstrated that the compound had high binding affinity for the insulin receptor, and the radiolabeled version was more stable in mouse plasma than $^{125}$I-insulin. Biodistribution studies in normal mice showed rapid clearance of the tracer in the urine, which was also observed in tumor models bearing insulin receptor positive tumors.

## EXPERIMENTAL PROCEDURES

**Materials and Instrumentation.** Chemicals were obtained from Sigma-Aldrich (Milwaukee, WI) and used without further purification while HPLC solvents were obtained from Caledon (Georgetown, ON, Canada). A Biotage V10 Evaporator (Uppsala, Sweden) was utilized in the radiosynthesis of the insulin derivatives. Purification and analysis of radioactive material by HPLC was performed on a Waters 1525 Binary HPLC system (Milford, MA) fitted with a Waters 2998 photodiode array detector and Bioscan gamma detector with NaI(T1) scintillator and either a semipreparative HPLC column (Phenomenex, Gemini-NX, C18, 5 $\mu$m, 110 Å, 10 × 250 mm) or an analytical HPLC column (Phenomenex, Gemini-NX, C18, 5 $\mu$m, 110 Å, 4.6 × 250 mm), respectively. For purification of nonradioactive material, HPLC was performed using a Varian Prostar HPLC system (Palo Alto, CA) fitted with a 330 PDA multiwavelength detector, a 230 solvent delivery module, and a semipreparative HPLC column (Phenomenex, Gemini-NX, C18, 5 $\mu$m, 110 Å, 10 × 250 mm). Absorbance was monitored at 254 nm. The mobile phase in all cases was derived from (A) $H_2O$ + 0.1% TFA and (B) $CH_3CN$ + 0.1% TFA. HPLC method A had a gradient profile of 80/20 to 30/70 A/B (v/v) over 22 min, 30/70 to 0/100 A/B over 3 min, followed by an isocratic wash of 0/100 A/B over 3 min, at a flow rate of 4 mL/min. Method B had a gradient profile of 75/25 to 20/80 A/B (v/v) over 20 min, 20/80 to 0/100 A/B over 3 min, followed by an isocratic wash of 0/100 A/B over 2 min at a flow rate of 1.0 mL/min. Method C had a gradient of 75/25 to 20/80 A/B (v/v) over 25 min at a flow rate of 1.0 mL/min. According to HPLC analysis, supported by NMR spectroscopy and HRMS where appropriate, the purity of all test compounds was >95%.

No-carrier-added [$^{18}$F]fluoride was produced by the $^{18}$O(p,n)$^{18}$F reaction by bombardment of an isotopically enriched $H_2$[$^{18}$O]O target using a Siemens RDS 112 cyclotron (Siemens CTI, Knoxville, TN) and obtained as a 1:1 v/v acetonitrile−water solution containing Kryptofix (K-222, 0.01992 mmol/mL) and $KHCO_3$ (0.03708 mmol/mL). Radioactivity was measured in a dose calibrator (Capintec, Ramsey, NJ) and a Wizard 1470 Automated Gamma Counter (PerkinElmer, Woodbridge, ON) for tissue distribution studies. Centrifugation was performed on a table top laboratory centrifuge International Clinical Centrifuge at approximately 1500 G.

*Animal Studies.* Animal studies were approved by the Animal Research Ethics Board at McMaster University in accordance with Canadian Council on Animal Care (CCAC) guidelines. All strains of mice were purchased from Charles River Laboratories (Senneville, QC) and were maintained under SPF conditions in an established animal facility with 12 h light/dark cycles and given food and water ad libitum.

**Synthetic Procedures.** *N-Succinimidyl-4-fluorobenzoate (*$^{19}$*F-**2a**).* 4-Fluorobenzoic acid (500 mg, 3.57 mmol) and *N*-hydroxysuccinimide (1.2 g, 10.42 mmol) were added to ethyl-3-(3-(dimethylamino)propyl)-carbodiimide hydrochloride (1.94 g, 10.12 mmol) in acetonitrile (40 mL), and the reaction mixture was stirred under nitrogen at room temperature for 4 h. The solvent was subsequently removed in vacuo and the residue redissolved in $CH_2Cl_2$ (300 mL). The organic layer was extracted with water (100 mL × 3), dried over anhydrous $MgSO_4$, and


dx.doi.org/10.1021/jm401020c | J. Med. Chem. XXXX, XXX, XXX−XXX

concentrated in vacuo. The product, a white solid (597 mg, 71%), was isolated by flash column chromatography (2:1 hexane−ethyl acetate). Characterization data matched that reported in the literature.[17]

*$A^1$,$B^{29}$-Di(tert-butyloxycarbonyl)insulin, DBI (**1**).* DBI was prepared by a previously reported procedure.[15b,c] Semiprep HPLC purification gave **1** (320 mg, 61%) as a white fluffy solid where characterization data matched that reported in the literature.

*$A^1$,$B^{29}$-Di(tert-butyloxycarbonyl)-$B^1$-(4-[$^{19}$F]fluorobenzoyl)insulin (**3a**).* DBI (10 mg, 1.67 $\mu$mol) and **2a** (8.2 mg, 0.035 mmol) were dissolved in DMSO (0.2 mL) containing 5% (v/v) $Et_3N$. After being stirred for 1.5 h at room temperature, the reaction mixture was poured into a centrifuge vial containing cold diethyl ether (2 mL) and $CH_3CN$ (2 mL), which induced precipitation. The solid was collected by centrifugation for 30 min at 3000 rpm (5 °C), and the resulting pellet was washed with 1:1 (v/v) diethyl ether/acetonitrile (1 mL). The product was subsequently isolated using semipreparative HPLC (method A). The desired fraction, which eluted between 10 and 11 min, was collected, and the solvents were removed using lyophilization, producing **3** as a white fluffy solid (6 mg, 57%). Analytical HPLC $t_R$ = 13.1 min (method B). MS (ESI) calculated: 1533.5, 2044.3, 6131; found: 1533.4 $[M + 4H^+]/4$, 2044.8 $[M + 3H^+]/3$, 6131 $[M + H^+]$.

*$B^1$-(4-Fluorobenzoyl)insulin ($^{19}$F-**4a**).* Trifluoroacetic acid (200 $\mu$L) and anisole (10 $\mu$L) were added to **3** (3 mg, 0.5 $\mu$mol), and the reaction mixture was stirred at room temperature for 30 min. The mixture was subsequently poured into a centrifuge vial containing cold diethyl ether (1 mL), which induced precipitation. The solid was collected by centrifugation at 3000 rpm (5 °C). The pellet was removed and dried under a stream of $N_2$ at room temperature. The product was isolated using semipreparative HPLC (method A) where the desired fraction eluted between 7.5 and 7.6 min, which was collected, and the solvents were removed using lyophilization. $^{19}$F-**4a** was isolated as a white fluffy solid in 69% yield (2 mg). HPLC $t_R$ = 11.8 min (method B). MS (ESI) calculated: 1187, 1483.5, 5931; found: 1187 $[M + 5H^+]/5$, 1483.7 $[M + 4H^+]/4$, 5931 $[M + H^+]$.

*Ethyl 4-Trimethylammonium Benzoate Trifluoromethanesulfonate (**5**).* Compound **5** was prepared following a literature procedure with some modification.[19] To ethyl 4-(dimethylamino)benzoate (300 mg, 1.55 mmol) in dichloromethane (17 mL) was added methyl trifluoromethanesulfonate (0.26 mL, 2.30 mmol), and the reaction mixture was stirred under nitrogen for 3 h at 60 °C. The solution was cooled and partitioned between diethyl ether (40 mL) and water (50 mL), and the aqueous layer was extracted again with diethyl ether (50 mL) and chloroform (50 mL). The combined organic layers were then concentrated in vacuo. Recrystallization from diethyl ether (7 mL) and ethanol (0.7 mL) afforded **5** as a white solid (487 mg, 88%). $^1$H NMR (600 MHz, DMSO) 8.16−8.11 (m, 4H), 4.36 (dd, 2H, $J$ = 7.1 Hz, $J$ = 7.1 Hz), 3.63 (s, 9H), 1.34 (t, 3H, $J$ = 7.1 Hz). $^{13}$C NMR (150 MHz, DMSO) 164.35, 150.43, 131.32, 130.68, 121.28, 61.39, 56.37, 14.06. MS (ESI) $m/z$ 208 $[M^+ - OTf]$; HRMS calculated for $C_{12}H_{18}NO_2$: 208.1332, found 208.1338.

*N-Succinimidyl 4-[$^{18}$F]Fluorobenzoate ($^{18}$F-**2b**).* K[$^{18}$F]F was dried by azeotropic distillation using acetonitrile three times (200 $\mu$L) at 90 °C under a gentle stream of $N_2$. DMSO (300 $\mu$L) was added, followed by **5** (5 mg, 0.014 mmol). The reaction mixture was heated to 90 °C for 10 min in a heating block where, after cooling to room temperature, 0.5 N NaOH (300 $\mu$L) was added and the mixture heated to 90 °C for 5 min. After cooling, the reaction mixture was neutralized with 1 N HCl (150 $\mu$L) and diluted with water (10 mL). The mixture was loaded onto a C18 SPE cartridge, previously activated with EtOH (10 mL), and then washed with water (10 mL). The crude product was eluted using acetonitrile (1.5 mL), and the solvent was evaporated under a stream of nitrogen at 90 °C. The residue was redissolved in acetonitrile (300 $\mu$L), and TSTU (10 mg, 0.033 mmol) was added as a solid. The reaction mixture was heated to 90 °C for 5 min, and the desired product isolated by semipreparative HPLC (method A). The fraction containing the product, which eluted between 12 and 13 min, was diluted with water (6 mL) and the resulting solution loaded onto a C18 SPE cartridge. The cartridge was washed with water (10 mL) prior to eluting the desired product $^{18}$F-**2b** with acetonitrile. After evaporation of the solvent using a Biotage V10eVaporator, the decay-corrected radiochemical yield of $^{18}$F-**2b** was 45 ± 6% ($n$ = 9) and the total synthesis time was 100 min including HPLC purification.

*$B^1$-(4-[$^{18}$F]Fluorobenzoyl)insulin ($^{18}$F-**4b**).* Purified $^{18}$F-**2b** in PBS buffer (pH 7.4, 100 $\mu$L) was added to a solution of $A^1$,$B^{29}$-Di-Boc-insulin (0.1 mg, 16.6 nmol) in 0.1 M $NaHCO_3$ (100 $\mu$L). Isooctane (1 mL) containing 1% v/v Span 80 was then added and the tube capped before vortexing for 3 s on the highest setting. The vortexed solution was then sonicated for 30 min with revortexing every 5 min. Afterward, trifluoroacetic acid (250 $\mu$L) containing anisole (10% v/v) was added and the solution shaken and then centrifuged at 3500 rpm for 10 min. The aqueous layer was collected and the product isolated by semipreparative HPLC using the same method as was described for $^{18}$F-**2b**. The desired fraction, which eluted between 7.5 and 8 min was collected, diluted with water (6 mL), and loaded onto a EtOH (10 mL) activated C18 SPE cartridge, which was then washed with water (10 mL) prior to eluting the product with acetonitrile (1.5 mL). The solvent was removed using a streaming of Ar gas at room temperature and the product reformulated with 0.9% normal saline. The decay-corrected radiochemical yield for the conjugation and deprotection reaction was 30 ± 10% ($n$ = 9), and the overall isolated yield including radiochemical synthesis of $^{18}$F-**2b** was 6% with a total synthesis time of 240 min. Typical reactions started with 3.7 GBq of fluoride and produced 48 MBq of the final product.

*In Vitro Insulin Receptor Competition Binding Assay with $^{125}$I-Insulin.* Three insulin receptor competition binding assays were conducted for $^{19}$F-**4a** and unlabeled recombinant human insulin (I2643, Sigma-Aldrich Canada Co., Oakville, ON) with each experimental measurement performed in triplicate. MCF-7 cells (ATCC HTB-22; Cedarlane Laboratories Ltd., Burlington, ON) were cultured in DMEM in the presence of 10% fetal bovine serum (FBS) and 1% penicillin−streptomycin (Invitrogen, Burlington, ON) at 37 °C, 5% $CO_2$. Cells were plated at a density of $1.0 \times 10^5$ or $1.5 \times 10^5$ cells per well in a 48 well plate 2 or 3 days (respectively) prior to the assay. Approximately 20 to 24 h prior to commencing the assay, the wells were rinsed twice with warm PBS and replaced with fresh DMEM containing 10% charcoal-stripped fetal bovine serum (csFBS; VWR, Mississauga, ON). Wells were rinsed once with warm PBS, and the cells were then incubated for 4 h at 4 °C with 150 $\mu$L of 1 nM $^{125}$I-insulin (human recombinant (NEX420); PerkinElmer)) in insulin receptor binding buffer (100 mM HEPES, 120 mM NaCl, 1.2 mM $MgSO_4$, 5 mM KCl, 15 mM Na acetate, 10 mM glucose, 1 mg/mL bovine serum albumin (BSA; all from Sigma-Aldrich Canada Co.) and 1 mg/mL bacitracin (BioShop Canada Inc., Burlington, ON) in the presence of 0 to 1000 nM cold competitor per well. To remove unbound ligand, wells were rinsed three times with ice-cold PBS, and cells were solubilized with 600 $\mu$L of 1 N NaOH at 37 °C for 30 min. A 500 $\mu$L sample from each well was collected in individual 12 × 55 mm Ria plastic test tubes (PerkinElmer) and counted for 10 min each using a gamma counter. The resulting CPM values were used to calculate the relative binding of each competition concentration with respect to the control run in the absence of a competitor. GraphPad Prism 5 software was used to analyze the data and determine the average $IC_{50}$ values.

*Western Blot Analysis of IR Expression.* CHO-K1 and CHO/HIRC cell lysates and tissue (Balb/c mouse liver or human tumor xenograft) homogenates were prepared using a lysis buffer composed of 1% NP-40 alternative, 20 mM Tris pH 8.0, 137 mM NaCl, 10% glycerol, 2 mM EDTA, 1 $\mu$M NaF, 1 $\mu$M Na orthovanadate, and 1X SIGMAFAST protease inhibitor cocktail without EDTA (Sigma-Aldrich Canada Co.). Protein concentrations of the lysates and homogenates were performed using the microplate procedure of the Pierce Microplate BCA Protein Assay Kit (Fisher Scientific, Ottawa, ON). Proteins were separated on a 10% SDS PAGE gel followed by transfer to PVDF membrane (BioRad, Mississauga, ON). The membranes were treated with Tris-buffered saline (pH 8.0) containing 0.1% Tween-20 and 5% milk powder and then incubated overnight at 4 °C with a 1:1000 dilution of an insulin receptor $\beta$ mouse monoclonal antibody (L55B10, Cell Signaling from NEB, Whitby, ON) in the same buffer. The insulin receptor specific bands were then visualized using an alkaline phosphatase conjugated goat antimouse secondary antibody (Jackson Laboratories, Bar Harbor, ME) and ECF Substrate with the Storm 840 Phosphor-Chemifluorescence Workstation (GE Healthcare Life Sciences, Baie d'Urfe QC). Relative densitometry of the insulin receptor bands were determined using


dx.doi.org/10.1021/jm401020c | J. Med. Chem. XXXX, XXX, XXX−XXX

ImageQuant 5.2 software and normalized to micrograms of protein loaded per lane.

*Cell Binding Studies with $^{125}$I-Insulin.* Cell binding studies ($n$ = 3) with multiple cell lines were conducted using $^{125}$I-insulin, $^{19}$F-**4a**, and recombinant human insulin. The assay was performed in triplicate for each condition using a modified version of the in vitro competition binding assay procedure described in this paper. MCF-7 and DU4475 cells (ATCC HTB-22 and ATCC HTB-123; Cedarlane Laboratories Ltd.) were cultured in DMEM in the presence of 10% FBS and 1% penicillin–streptomycin (Invitrogen, Burlington, ON) at 37 °C and 5% $CO_2$. CHO-K1 (ATCC CCL-61; Cedarlane Laboratories Ltd.) and CHO/HIRC cells, a Chinese hamster ovary cell line stably transfected with the human insulin receptor isoform B that was a generous gift from Dr. Jonathan M. Backer (Albert Einstein College of Medicine, New York), were propagated using Ham's F-12 media supplemented with 10% FBS and 1% penicillin–streptomycin (Invitrogen, Mississauga, ON) and grown at 37 °C and 5% $CO_2$. Adherent cells were plated at a density of $1.0 \times 10^5$ or $1.5 \times 10^5$ cells per well for MCF-7 cells and $7.5 \times 10^4$ or $3.25 \times 10^4$ cells per well for both CHO cell lines in a 48-well plate 2 and 3 days, respectively, prior to the assay. Approximately 20 to 24 h prior to commencing the assay the wells were rinsed twice with warm PBS and replaced with appropriate fresh medium containing 10% charcoal stripped fetal bovine serum (csFBS; VWR, Mississauga, ON). Because DU4475 cells grow in suspension, these cells were washed twice with warm PBS and resuspended with fresh medium containing 10% csFBS in a tissue culture flask.

Prior to incubation with $^{125}$I-insulin, cells (adherent or suspension) were rinsed once with warm PBS. Rinsed DU4475 cells were counted, and $1.5 \times 10^5$ cells were placed in 1.5 mL microcentrifuges tubes. Cells (adherent or suspension) were then incubated for 4 h at 4 °C with 150 μL of 0.1 nM or 1 nM $^{125}$I-insulin (human recombinant (NEX420) in insulin receptor binding buffer in the presence or absence of 1000 nM cold competitor per well. The DU4475 cell containing tubes were rotated to prevent cells from pelleting. To remove unbound ligand, cells were rinsed three times with ice-cold PBS and solubilized with 600 μL of 1 N NaOH at 37 °C for 30 min. A 500 μL sample from each lysate was transferred to 12 × 55 mm Ria plastic test tubes (PerkinElmer) and counted for 10 min using a gamma counter. Control cells (treated identically but with no radioactivity) were harvested with 0.25% trypsin with EDTA (Invitrogen, Mississauga, ON), resuspended in 10% FBS containing medium and counted to get an average cell number per well or tube. For each cell line, the resulting CPM values were then normalized by cell number to give a relative average CPM per cell.

*Stability of $^{18}$F-**4b** in Mouse Plasma.* Plasma stability was examined for $^{18}$F-**4b** in collected and pooled CD-1 mouse plasma from fasted animals of mixed sex (Cedarlane Laboratories Ltd.). At room temperature, 230 μL (11.1 MBq) of $^{18}$F-**4b** formulated in saline was mixed with 230 μL of plasma or 0.9% saline, as the control, in a 1.5 mL microcentrifuge tube, and the mixtures were incubated at 37 °C. Aliquots of 100 μL were removed at various time points ($t$ < 1, 5, 15, and 30 min) and mixed well with 200 μL of ice-cold acetonitrile. The precipitate was isolated by centrifugation at room temperature (~21 000$g$ for 10 min), and the supernatant was collected and transferred to a clean glass vial containing 600 μL of 0.9% saline for HPLC analysis (method C).

*Biodistribution Study of $^{18}$F-**4b** in Balb/c Mice.* Biodistribution of $^{18}$F-**4b** was performed using 6–7 week old female Balb/c mice ($N$ = 5 per time point at $t$ = 5, 30, 60, 180 min). The mice were administered ~0.91 MBq of $^{18}$F-**4b** (100 μL in PBS) via tail vein injection, and animals were anesthetized with 3% isoflurane and euthanized by cervical dislocation. Blood, heart, lungs, liver, gall bladder, spleen, kidneys, adrenals, pancreas, stomach (with contents), small intestine (with contents), large intestine and cecum (with contents), white adipose, brown adipose, thyroid/trachea, bone, skeletal muscle, brain, bladder and urine, and tail were collected, weighed, and counted in an automated gamma counter. Decay correction was used to normalize organ activity measurements to time of dose preparation for data calculations with respect to injected dose (i.e., %ID/g).

*CHO/HIRC Tumor Xenograft Model.* To create a tumor xenograft model, CD-1 nude homo female mice were injected with $2.0 \times 10^6$ CHO/HIRC cells in 100 μL of Matrigel/DPBS (1:1; BD Biosciences, Mississauga, ON, and Invitrogen, Burlington, ON, respectively) subcutaneously into the right flank at 4 to 5 weeks of age. Tumors were allowed to grow for approximately 2 weeks before animals were used in biodistribution studies.

*Biodistribution Study of $^{18}$F-**4b** in Tumor-Bearing Mice.* Biodistribution studies of $^{18}$F-**4b** were performed using CD-1 nu homo mice bearing 14 day old CHO/HIRC tumors. The mice were administered ~0.68 MBq of $^{18}$F-**4b** (100 μL in PBS) via tail vein injection. Animals were sacrificed at 5 and 30 min, whereupon tumor and tissues were isolated and samples were processed and analyzed as described for the biodistribution studies involving Balb/c mice.

*Biodistribution Study of $^{125}$I-Insulin in Tumor-Bearing Mice.* Biodistribution of $^{125}$I-insulin (human recombinant (NEX420)) was performed on CD-1 nu homo mice bearing 14 day old CHO/HIRC tumors ($n$ = 4 at 5 and 60 min and $n$ = 5 at 30 min). Lyophilized $^{125}$I-insulin was reconstituted with sterile $dH_20$ (Invitrogen, Burlington, ON) as per PerkinElmer Certificate of Analysis and then diluted with 0.5 volumes of sterile injectable USP 0.9% NaCl (Hospira, Saint-Laurent QC). The mice were administered ~0.27 MBq in 150 μL via tail vein injection, animals sacrificed, tumor and tissues isolated, and samples processed and analyzed as described for the studies involving Balb/c mice.

## ■ ASSOCIATED CONTENT

### Ⓢ Supporting Information

$^1$H, $^{13}$C, and MS spectra, HPLC traces, $^{125}$I-IGF-1 in vitro assay methods and results, and biodistribution data. This material is available free of charge via the Internet at http://pubs.acs.org

## ■ AUTHOR INFORMATION

### Corresponding Author

*Tel: 905-525-9140 ext. 20182. Fax: 905-522-2509. E-mail: valliant@mcmaster.ca.

### Notes

The authors declare no competing financial interest.

## ■ ACKNOWLEDGMENTS

The authors thank the Canadian Cancer Society Research Institute (CCSRI) and the Ontario Institute for Cancer Research (OICR) for their financial support of this work, and Prof. Jonathan M. Backer (Albert Einstein College of Medicine, New York) for his a generous and appreciated gift of the Chinese hamster ovary cell line stably transfected with the human insulin receptor isoform B.

## ■ ABBREVIATIONS USED

DBI, A$^1$,B$^{29}$-di(*tert*-butyloxycarbonyl)insulin; IGF-1R, insulin-like growth factor-1 receptor; IR, insulin receptor; SFB, *N*-succinimidyl-4-fluorobenzoate; %ID/g, percent injected dose per gram

## ■ REFERENCES

(1) Banting, F. G.; Best, C. H. The internal secretion of the pancreas. *J. Lab. Clin. Med.* **1922**, *7*, 464–472.

(2) Saltiel, A. R.; Kahn, C. R. Insulin signaling and the regulation of glucose and lipid metabolism. *Nature* **2001**, *414*, 799–806.

(3) DeFronzo, R. A. Insulin resistance: a multifaceted syndrome responsible for NIDDM, obesity, hypertension, dyslipidaemia and atheriosclerosis. *Neth. J. Med.* **1997**, *5*, 191–197.

(4) Paternostro, G.; Pagano, D.; Gnecchi-Ruscone, T.; Bonser, R. S.; Camici, P. G. Insulin resistance in patients with cardiac hypertrophy. *Cardiovasc. Res.* **1999**, *42*, 246–253.

(5) Hoyer, S. Is sporadic Alzheimer disease the brain type of non-insulin dependent diabetes mellitus? A challenging hypothesis. *J. Neural Transm.* **1998**, *105*, 415–422.

(6) (a) Osborne, C. K.; Monaco, M. W.; Lippman, M. E.; Kahn, C. R. Correlation among insulin binding, degredation, and biological activity in human breast cancer cells in long-term tissue culture. *Cancer Res.* **1978**, *38*, 94−102. (b) Kaaks, R.; Toniolo, P.; Akhmedkhanov, A.; Lukanova, A.; Biessy, C.; Dechaud, H.; Rinaldi, S.; Zeleniuch-Jacquotte, A.; Shore, R. E.; Riboli, E. Serum C-peptide, insulin-like growth factor (IGF)-I IGF-binding proteins, and colorectal cancer risk in women. *J. Natl. Cancer Inst.* **2000**, *92*, 1592−1600. (c) Belfiore, A.; Malaguarnera, R. Insulin receptor and cancer. *Endocr.-Relat. Cancer* **2011**, *18*, R125−R147. (d) Belfiore, A.; Frasca, F.; Pandini, G.; Sciacca, L.; Vigneri, R. Insulin receptor isoforms and insulin receptor/insulin-like growth factor receptor hybrids in physiology and disease. *Endocr. Rev.* **2009**, *30*, 586−623.

(7) (a) Koontz, J. W.; Iwahashi, M. Insulin as a potent, specific growth factor in rat hepatoma cell line. *Science* **1981**, *211*, 947−949. (b) Massague, J.; Blinderman, L. A.; Czech, M. P. The high affinity insulin receptor mediates growth stimulation in rat hepatoma cells. *J. Biol. Chem.* **1982**, *257*, 3958−3963.

(8) (a) Frittitta, L.; Cerrato, A.; Sacco, M. G.; Weidner, N.; Goldfine, I. D.; Vigneri, R. The insulin receptor content is increased in breast cancers initiated by three different oncogens in transgenic mice. *Breast Cancer Res. Treat.* **1997**, *45*, 141. (b) Belfiore, A.; Frittitta, L.; Costantino, A.; Frasca, F.; Pandini, G.; Sciacca, L.; Goldfine, I. D.; Vigneri, R. Insulin receptors in breast cancer. *Ann. N.Y. Acad. Sci.* **1996**, *784*, 173−188. (c) Webster, N. J. G.; Resnik, J. L.; Reichart, D. B.; Strauss, B.; Haas, M.; Seely, B. L. Repression of the insulin receptor promoter by the tumor suppressor gene product p53: a possible mechanism for receptor overexpression in breast cancer. *Cancer Res.* **1996**, *56*, 2781−2788. (d) Mulligan, A. M.; O'Mally, F. P.; Ennis, M.; Fantus, G.; Goodwin, P. J. Insulin receptor is an independent predictor of a favorable outcome in early stage breast cancer. *Breast Cancer Res. Treat.* **2007**, *106*, 39−47. (e) Novosyadlyy, R.; Lann, D. E.; Vijayakumar, A.; Rowzee, A.; Lazzarino, D. A.; Fierz, Y.; Carboni, J. M.; Gottardis, M. M.; Pennisi, P. A.; Molinolo, A. A.; Kurshan, N.; Mejia, W.; Santopietro, S.; Yakar, S.; Wood, T. L.; LeRoith, D. Insulin-mediated acceleration of breast cancer development and progression in a nonobese model of type 2 diabetes. *Cancer Res.* **2010**, *70*, 741−51. (f) Zhang, H.; Pelzer, A. M.; Kiang, D. T.; Yee, D. Down-regulation of type I insulin-like growth factor receptor increases sensitivity of breast cancer cells to insulin. *Cancer Res.* **2007**, *67*, 391−397. (g) Papa, V.; Pezzino, V.; Costantino, A.; Belfiore, A.; Giuffrida, D.; Frittitta, L.; Vannelli, G. B.; Brand, R.; Goldfine, I. D.; Vigneri, R. Elevated insulin receptor content in human breast cancer. *J. Clin. Invest.* **1990**, *86*, 1503−1510.

(9) Ulanet, D. B.; Ludwig, D. L.; Kahn, C. R.; Hanahan, D. Insulin receptor functionally enhances multistage tumor progression and conveys intrinsic resistance to IGF-1R targeted therapy. *Proc. Nat. Acad. Sci. U.S.A.* **2010**, *107*, 10791−10798.

(10) (a) Baserga, R. The decline and fall of the IGF-I receptor. *J. Cell. Physiol.* **2013**, *228*, 675−679. (b) Zhang, Y.; Cai, W. Molecular imaging of insulin-like growth factor 1 receptor in cancer. *Am. J. Nucl. Med. Mol. Imaging* **2012**, *2*, 248−259. (c) Pollak, M. Insulin and insulin-like growth factor signalling in neoplasia. *Nat. Rev. Cancer* **2008**, *8*, 915−928. (d) Siddle, K. Signalling by insulin and IGF receptors: Supporting acts and new players. *J. Mol. Endocrinol.* **2011**, *47*, R1−R10.

(11) (a) Haluska, P.; Carboni, J. M.; Loegering, D. A.; Lee, F. Y.; Wittman, M.; Saulnier, M. G.; Frennesson, D. B.; Kalli, K. R.; Conover, C. A.; Attar, R. M.; Kaufmann, S. H.; Gottardis, M.; Erlichman, C. *In vitro* and *in vivo* antitumor effects of the dual insulin-like growth factor-I/insulin receptor inhibitor, BMS-554417. *Cancer Res.* **2006**, *66*, 362−371. (b) Law, J. H.; Habibi, G.; Hu, K.; Masoudi, H.; Wang, M. Y. C.; Stratford, A. L.; Park, E.; Gee, J. M. W.; Finlay, P.; Jones, H. E.; Nicholson, R. I.; Carboni, J.; Gottardis, M.; Pollak, M.; Dunn, S. E. Phosphorylated insulin-like growth factor-I/insulin receptor is present in all breast cancer subtypes and is related to poor survival. *Cancer Res.* **2008**, *68*, 10238−10246. (c) Sachdev, D.; Singh, R.; Fujita-Yamaguchi, Y.; Yee, D. Down-regulation of insulin receptor by antibodies against the type I insulin-like growth factor receptor: Implications for anti-insulin-like growth factor therapy in breast cancer. *Cancer Res.* **2006**, *66*, 2391−2402.

(12) (a) Wajchenberg, B. L.; Pinto, H.; Torres de Toledo e Souza, I.; Lerario, A. C.; Pieroni, R. R. Preparation of iodine-125-labeled insulin for radioimmunoassay: Comparison of lactoperoxidase and chloramine-T iodination. *J. Nucl. Med.* **1978**, *19*, 900−905. (b) Jorgensen, K. H.; Larsen, U. D. Homogenous mono[$^{125}$I] insulins: Preparation and characterization of mono-[$^{125}$I]-(Tyr A14)- and mono-[$^{125}$I]-(Tyr A19)-insulin. *Diabetologica* **1980**, *19*, 546−554. (c) Rissler, K.; Engelmann, P. Labeling of insulin with non-radioactive $^{127}$I and application to incorporation of radioactive $^{125}$I for use in receptor binding experiments by high-performance liquid chromatography. *J. Chromatogr., Biomed. Appl.* **1996**, *679*, 21−29.

(13) (a) Kurtaran, A.; Li, S. R.; Raderer, M.; Leimer, M.; Müller, C.; Pidlich, J.; Neuhold, N.; Hübsch, P.; Angelberger, P.; Scheithauer, W.; Virgolini, I. Technetium-99m-galactosyl-neoglycoalbumin combined with iodine-123-tyr-(A14)-insulin visualizes human hepatocellular carcinomas. *J. Nucl. Med.* **1995**, *36*, 1875−1881. (b) Hachiya, H. L.; Treves, S. I.; Kahn, C. R.; Sodoyez, J. C.; Sodoyez-Goffaux, F. Altered insulin distribution and metabolism in type I diabetics assessed by [$^{123}$I] insulin scanning. *J. Clin. Endocrinol. Metab.* **1987**, *64*, 801−808. (c) Sodoyez, J. C.; Sodoyez-Goffaux, F.; Guillaume, M.; Merchie, G. [$^{123}$I]-Insulin metabolism in normal rats and humans. External detection by a scintillation camera. *Science* **1983**, *219*, 865−867.

(14) (a) Glaser, M.; Brown, D. J.; Law, M. P.; Iozzo, P.; Waters, S. L.; Poole, K.; Knickmeier, M.; Camici, P. G.; Pike, V. W. Preparation of no-carrier-added [$^{124}$I]A14-iodoinsulin as a radiotracer for positron emission tomography. *J. Labelled Compd. Radiopharm.* **2001**, *44*, 465−480. (b) Iozzo, P.; Osman, S.; Glaser, M.; Knickmeier, M.; Ferrannini, E.; Pike, V. W.; Camici, P. G.; Law, M. P. *In vivo* imaging of insulin receptors by PET: preclinical evaluation of iodine-125 and iodine-124 labelled human insulin. *Nucl. Med. Biol.* **2002**, *29*, 73−82.

(15) (a) Eastman, R. C.; Carson, R. E.; Jacobson, K. A.; Shai, Y.; Channing, M. A.; Dunn, B. B.; Bacher, J. D.; Baas, E.; Jones, E.; Kirk, K. L.; Lesniak, M. A.; Roth, J. *In vivo* imaging of insulin receptors in monkeys using $^{18}$F-labelled insulin and positron emission tomography. *Diabetes* **1992**, *41*, 855−860. (b) Shai, Y.; Kirk, K. L.; Channing, M. A.; Dunn, B. B.; Lesniak, M. A.; Eastman, R. C.; Finn, R. D.; Roth, J.; Jacobson, K. A. $^{18}$F-Labeled insulin: a prosthetic group methodology for incorporation of a positron emitter into peptides and proteins. *Biochemistry* **1989**, *28*, 4801−4806. (c) Guenther, K. J.; Yoganathan, S.; Garofalo, R.; Kawabata, T.; Strack, T.; Labiris, R.; Dolovich, M.; Chirakal, R.; Valliant, J. F. Synthesis and in vitro evaluation of $^{18}$F- and $^{19}$F-labeled insulin: A new radiotracer for PET-based molecular imaging studies. *J. Med. Chem.* **2006**, *49*, 1466−1474.

(16) Sundararajan, C.; Besanger, T. R.; Labiris, R.; Guenther, K. J.; Strack, T.; Garafalo, R.; Kawabata, T. T.; Finco-Kent, D. F.; Zubieta, J.; Babich, J. W.; Valliant, J. F. Synthesis and characterization of rhenium and technetium-99m labeled insulin. *J. Med. Chem.* **2010**, *53*, 2612−2621.

(17) (a) Wester, H.-J.; Hamacher, K.; Stöcklin, G. A comparative study of N.C.A. fluorine-18 labeling of proteins via acylation and photochemical conjugation. *Nucl. Med. Biol.* **1996**, *23*, 365−372. (b) Kuchar, M.; Pretze, M.; Kniess, T.; Steinbach, J.; Pietzsch, J.; Loser, R. Site-selective radiolabeling of peptides by (18)F-fluorobenzoylation with [(18F)]SFB in solution and on solid phase: a comparative study. *Amino Acids* **2012**, *43*, 1431−1443.

(18) Chen, Y.; Pullambhatla, M.; Foss, C. A.; Byun, Y.; Nimmagadda, S.; Srinivasan, S.; Sgouros, G.; Mease, R. C.; Pomper, M. G. 2-(3-{1-Carboxy-5-[(6-[$^{18}$F]fluoro-pyridine-3-carbonyl)-amino]-pentyl}-ureido)-pentanedioic acid, [$^{18}$F]DCFPyL, a PSMA-based PET imaging agent for prostate cancer. *Clin. Cancer Res.* **2011**, *17*, 7645−7653.

(19) Haka, M. S.; Kilbourn, M. R.; Watkins, G. L.; Toorongian, S. A. Aryltrimethylammonium trifluoromethanesulfonates as precursors to aryl [$^{18}$F]fluorides: improved synthesis of [$^{18}$F]GBR-13119. *J. Labelled Compd. Radiopharm.* **1989**, *27*, 823−833.

(20) Simms, R. W.; Kim, D. H.; Weaver, D. M.; Sundararagan, C.; Blacker, M.; Stephenson, K. A.; Valliant, J. F. Emulsion reactors: a new technique for the preparation of molecular imaging probes. *Chem.—Eur. J.* **2012**, *18*, 6746−6749.

(21) Sodoyez, J. C.; Sodoyez-Goffaux, F. R.; Moris, Y. M. 125I-insulin: kinetics of interaction with its receptors and rate of degredation in vivo. *Am. J. Physiol. Endocrinol. Metab.* **1980**, *239*, E3−E8.